

Status of advanced ground-based laser interferometers for gravitational-wave detection

K L Dooley¹, T Akutsu², S Dwyer³, P Puppo⁴

¹ Max-Planck-Institut für Gravitationsphysik (Albert-Einstein-Institut) und Leibniz Universität Hannover, Callinstr. 38, D-30167 Hannover, Germany.

² National Astronomical Observatory of Japan, 2-21-1 Osawa, Mitaka, Tokyo 181-8588

³ LIGO Hanford Observatory, PO Box 159, Richland, WA 99352, USA

⁴ INFN, Sezione di Roma, I-00185 Roma, Italy

E-mail: kate.dooley@aei.mpg.de

Abstract. Ground-based laser interferometers for gravitational-wave (GW) detection were first constructed starting 20 years ago and as of 2010 collection of several years' worth of science data at initial design sensitivities was completed. Upgrades to the initial detectors together with construction of brand new detectors are ongoing and feature advanced technologies to improve the sensitivity to GWs. This conference proceeding provides an overview of the common design features of ground-based laser interferometric GW detectors and establishes the context for the status updates of each of the four gravitational-wave detectors around the world: Advanced LIGO, Advanced Virgo, GEO 600 and KAGRA.

1. Introduction

This is an exciting time for the maturing field of gravitational wave (GW) physics. The network of ground-based laser interferometer GW detectors (GWD) is making rapid progress towards its goal of producing advanced instruments sensitive enough to make monthly GW detections in the 10 Hz to 10 kHz frequency range by the end of the decade [1]. Simultaneously, there has recently been a claim by the BICEP2 experiment that the measurement of the B-modes in the cosmic microwave background polarization can be the signature of the primordial GWs produced by inflation [2]. If confirmed, this would add to the original evidence for GWs from 1975 by Hulse and Taylor who observed that the rate of change of the orbital period of a binary star system precisely agrees with the predictions of GR [3, 4]. Moreover, the eLISA space-based gravitational wave detector [5] together with the promising pulsar timing technique [6] will be very important in the coming decades for the investigation of very massive objects and other GW sources in the milli- to micro-Hz frequency ranges, respectively.

GWs are dynamic strains in space-time that travel at the speed of light and are generated by non-axisymmetric acceleration of mass. They perturb the flat Minkowski metric describing space-time. The effect is the production of a dimensionless strain between two inertial masses located at a proper distance L from one another so that their distance changes as:

$$\Delta L(t) = \frac{1}{2} L h(t) \quad (1)$$

¹ Current address: The University of Mississippi, University, MS 38677, USA



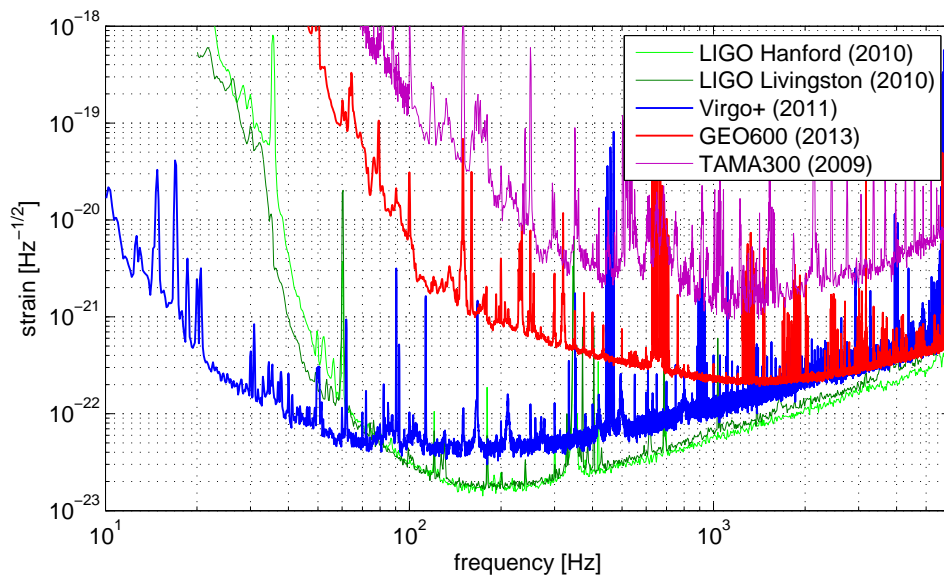


Figure 1. Strain sensitivities achieved by the first generation detectors.

In the late 20th century following the era of the operation of bar detectors for GW detection [7], large laser interferometers were identified as the promising route forward because of the very high strain sensitivities that could be achieved over a wide frequency band. R. Weiss produced the first detailed design study in 1972 of a large scale laser interferometer for GW detection, complete with calculations of fundamental noise sources [8]. Then, following the work of Forward [9] who built the first laser interferometric GW detector prototype, many groups around the world proceeded to study the benefits of laser interferometry, build new prototypes, perfect the design, and push technology development [10, 11, 12, 13].

The LIGO detectors in the U.S. [14], the Virgo detector in Italy [15], the GEO 600 detector in Germany [16] and the TAMA 300 [17] detector in Japan formed the first generation laser-interferometric GWD network. Construction of these projects began in the mid-1990s and then progressed in sequential commissioning and data-taking phases in the 2000s. These first-generation detectors achieved their original instrument sensitivity goals and are now undergoing major hardware upgrades to expand thousand-fold the observable volume of the cosmos. The strain sensitivities achieved by these initial detectors is shown in Figure 1. This paper describes the common design basics of the detectors and provides an overall summary of the current status of the worldwide network of GWDs, including a timeline for operations. The next four proceedings focus on the particular features and individual status of each of the advanced versions of these detectors [18, 19, 20, 21].

2. Background

A direct detection of gravitational waves themselves has not yet been made, but this is also not a surprise. The rate estimates for coalescing binary neutron stars, for instance, predict a detection probability of one event in 100 years for the initial detector sensitivities [1]. About two years' worth of double-coincidence data were collected. Nonetheless, the LIGO and Virgo collaborations have already produced astrophysical results from the data collected thus far. They have placed an upper limit that beats previous best estimates of the fraction of spin-down power emitted in GWs from the Crab Pulsar [22]. They have also placed an upper limit at 100 Hz on the normalized energy density of the stochastic GW background of cosmological and

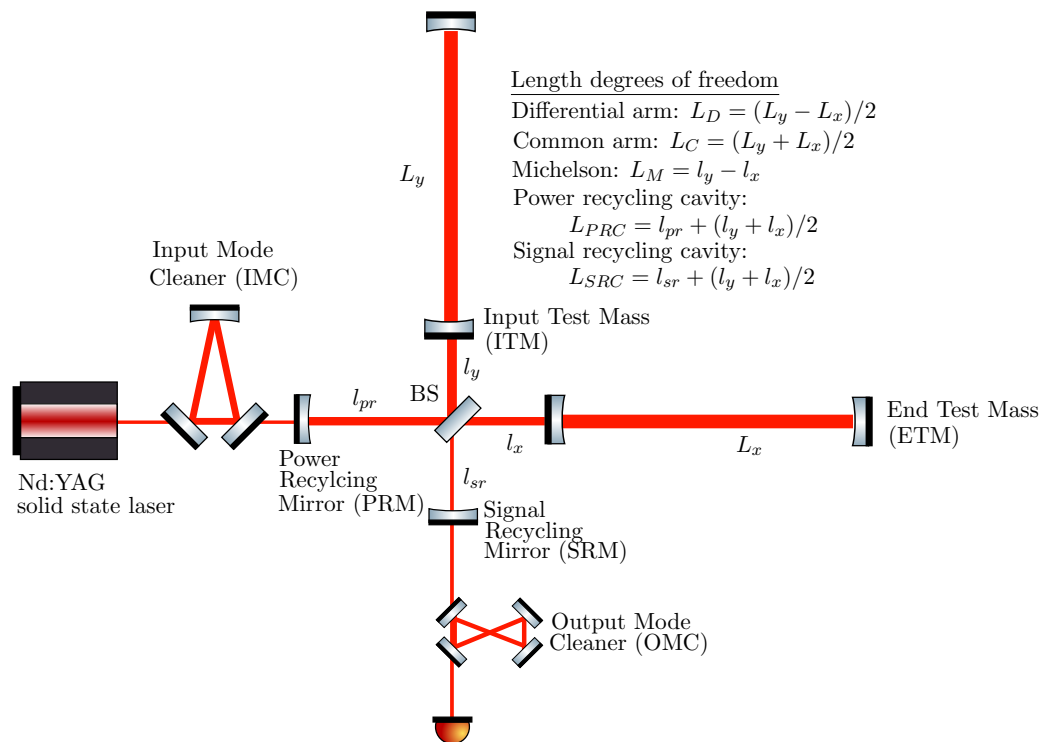


Figure 2. Layout of advanced ground-based interferometric gravitational wave detectors (not to scale). To keep the interferometer in its linear operating range, the length sensing and control system must control five interferometer length degrees of freedom and keep both mode cleaner cavities on resonance. The differential arm degree of freedom is sensitive to gravitational waves, and is sensed by the photo-detector in transmission of the output mode cleaner. GEO 600 is the exception in that it has no arm cavities.

astrophysical origin, a result otherwise inaccessible to standard observational techniques [23].

The last decade brought great advances in demonstrating the experimental feasibility of achieving the strain sensitivities required to witness astrophysical events and informed the design of today's generation of GWDs. Both LIGO and Virgo are re-using the infrastructure from the initial generation detectors and are replacing the hardware within the vacuum system. The upgraded detectors are called Advanced LIGO [24] and Advanced Virgo [25], respectively. TAMA 300 as well as CLIO, a prototype cryogenic laser interferometer [26], informed the design of a brand new detector called KAGRA, the first underground, cryogenic laser interferometer [27, 28]. GEO 600 is keeping its infrastructure and most of its initial generation hardware, but is carrying out upgrades to demonstrate advanced techniques in a program called GEO-HF [29]. In addition, a proposal to expand LIGO's baseline by building an interferometer in India is moving forward.

3. Detector design overview

The typical advanced detector configuration is that of a dual-recycled Fabry-Perot Michelson (DRFPM) laser interferometer as depicted in Figure 2. A power amplified, and intensity and frequency stabilized Nd:YAG solid state laser system injects linear-polarized 1064 nm light into a triangular input mode-cleaner (IMC) cavity. The IMC suppresses laser frequency noise and provides spatial filtering of the laser beam to reduce beam jitter that could otherwise couple to the GW readout. A beam splitter (BS) sends the beam to the two Fabry-Perot arms, which

are made of an input test mass mirror (ITM) and an end test mass mirror (ETM). Both arms are of km-scale lengths and are set to maintain nearly perfect destructive interference of the recombined light at the anti-symmetric (AS) port which carries the GW information. Here, the beam is directed to an output mode-cleaning (OMC) cavity and then onto a photo-detector. The OMC transmits only the signal-carrying light to improve the signal-to-noise ratio.

A power recycling mirror at the symmetric port directs the constructively-interfered light back into the interferometer. The transmissivity of the power recycling mirror is set to match the losses of the main optics to create a nearly critically coupled cavity. A signal recycling mirror at the anti-symmetric port creates an additional cavity which can be used to adjust the storage time of the gravitational wave signal in the interferometer and thus the frequency response of the detector. The signal recycling mirror has a transmissivity selected to compromise between high and low frequency sensitivity based on thermal noise and laser power. Until a few years ago all detectors used heterodyne readout. Since approximately 2008 as part of intermediary upgrades to the initial detectors [30], homodyne (*DC*) readout was implemented together with the addition of an OMC [31, 32].

Nearly the entire interferometer is enclosed in an ultra high vacuum (UHV) system to render phase noise of residual gas unimportant and to keep the optics free of dust. The primary interferometer optics are suspended as pendulums to decouple them from ground motion so that they act like free masses in the horizontal plane at the frequencies in the GW detection band. To minimize the impact of thermal noise, the mirror suspensions are designed to minimize dissipation and, in the case of KAGRA, operated at cryogenic temperatures. Each mirror is equipped with actuators for coarse and fine control of the mirror position and orientation.

A feedback control system is implemented to hold the system sufficiently near the intended operating point so that the response to residual deviations remains linear. Calibration of the detector must take into account the action of the control system and the frequency response of the detector [33]. The various length (illustrated in Figure 2) and angular degrees of freedom are sensed through the use of radio-frequency sidebands on the carrier light that are created through phase modulation by electro-optic modulators. The differential arm length signal is sensitive to gravitational waves, and is sensed using homodyne readout in transmission of the OMC, where the GW signal is encoded as power variations of the light. The standard technique for locking optical cavities is the Pound–Drever–Hall method of laser frequency stabilization [34]. Although the interferometer is an analog instrument, it is interfaced through a digital control system which allows complex filters to be implemented and tuned from the control room.

The sources of noise that contaminate the detector's output can be grouped into two categories: displacement noise and sensing noise. Displacement noises are those that create real motion of the mirrors, while sensing noises are those that arise in the process of measuring the mirrors' position. The primary displacement noise that plagues terrestrial laser interferometers at very low frequencies is motion of the ground, i.e. seismic noise. Thermal motion of the mirrors, their dielectric coatings and suspensions as well as quantum radiation pressure noise are the other two types of displacement noise which dominate in the low- to mid-frequency range [35]. The primary sensing noise is shot noise that arises from the Poisson statistics of photon arrival at the photodetector.

Figure 3 shows the spectra of these ultimate limits to the performance of each of the GW detectors in the advanced detector network. Each curve reflects the incoherent sum of fundamental noise sources, which gives a likely best limit to performance. The actual sensitivity will depend also on technical noise sources. The narrow lines in each of the noise curves represent the thermally-excited violin modes of the test mass suspension fibers. Quantum noise and thermal noise play the dominant roles in limiting the sensitivity of each of the detectors. The frequency at which there is a dip in the noise together with the shapes of the noise curves are largely affected by the signal recycling parameters, which may be adjusted during the course of

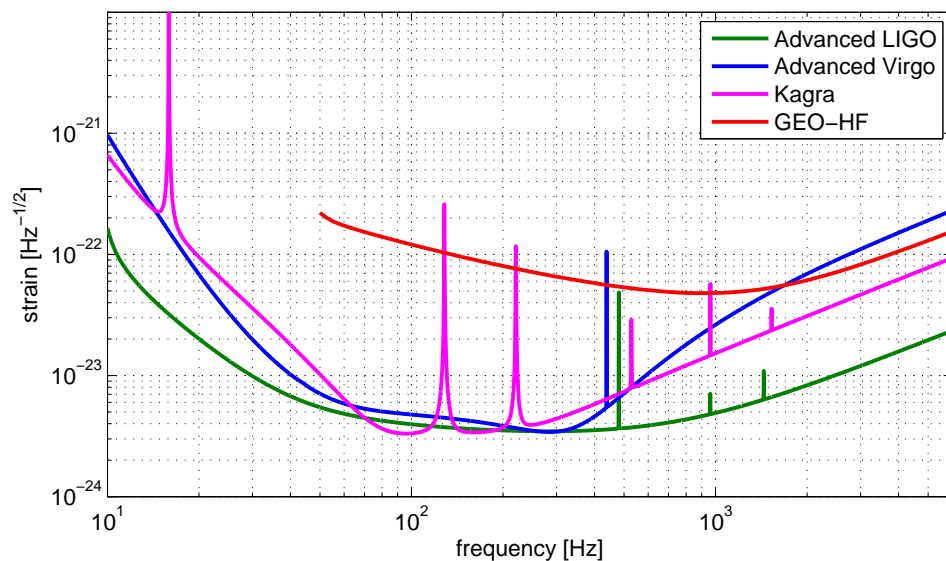


Figure 3. Prediction of the incoherent sum of fundamental noise sources which give a likely best limit to the performance of each of the instruments in the advanced detector network. Noise curves for both Advanced Virgo and KAGRA show a de-tuned signal recycling configuration optimized for sensitivity to neutron star binaries [25, 27, 36], whereas the Advanced LIGO and GEO-HF noise curves are shown with zero de-tuning [37, 38].

Table 1. Some design properties of each of the four GWDs. DRFPMI stands for dual-recycled Fabry-Perot Michelson.

	Advanced LIGO	Advanced Virgo	GEO-HF	KAGRA
arm length	4 km	3 km	2×600 m	3 km
power recycling gain	44	39	900	11
arm power	800 kW	700 kW	20 kW	400 kW
# of pendulum stages	4	8	3	6
mirror mass	40 kg	42 kg	6 kg	23 kg
mirror material	fused silica	fused silica	fused silica	sapphire
temperature	room	room	room	cryogenic
topology	DRFPMI	DRFPMI	DRMI	DRFPMI

operation of the advanced detectors. We postpone the detailed description of each noise curve to the proceedings dedicated to each detector. Table 1 provides an overview comparing some of the major properties of each of the detector designs.

4. Outlook

The advanced detectors form a four-site network which is crucial for GW signal characterization. The sky coverage depends on the detector locations and orientations. The two LIGO detectors are nearly aligned for maximum correlation, but they are relatively close together which results in signals that have largely redundant information about the source direction and character. For this reason, only the four-site network can provide full sky coverage [39].

Another important feature of a detector network is sky localization for electro-magnetic follow ups and multi-messenger investigations. In the case of signals from coalescing binary neutron

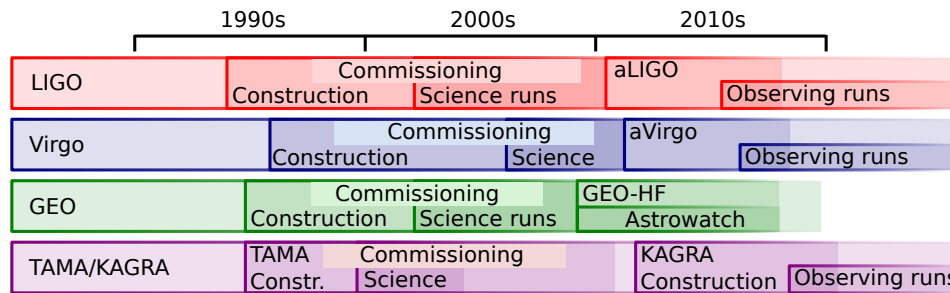


Figure 4. Timeline showing the approximate dates for construction, commissioning and science runs of each of the ground based GWDs. The first joint science runs in the advanced detector era are expected to begin taking place by late 2015.

star systems, the two Advanced LIGO detectors, Advanced Virgo, and KAGRA would provide a localization accuracy of 10 deg^2 for 50 % of the sources, while a five site network, including LIGO India, would improve the accuracy to 5 deg^2 for 30 % of the sources [40, 41]. This network of GW detectors together with the joint detection of the electro-magnetic counterparts is poised to open a promising window to gravitational wave astronomy.

Figure 4 shows a timeline of the construction, commissioning, and science run stages of each of the GWDs. The down times for each of the detectors is a bit staggered, with GEO 600 serving the role of being the sole detector online for the entirety of the period when the other detectors are offline. Commissioning and science run stages of the advanced detectors will be interspersed to allow for possible early results once astrophysically interesting sensitivities are reached, but before design sensitivity is reached [42]. The early science runs are likely to start in late 2015 with the Advanced LIGO detectors, and Advanced Virgo and KAGRA will join in due time.

Together with the promise of continuing to add to the collection of upper limits on GW emission in the era of advanced detectors, the first direct detection of GWs is expected to be made in only a couple years' time from now. A first detection is expected to witness an event such as a binary neutron star coalescence [1].

Acknowledgements

The authors gratefully acknowledge the support of the United States National Science Foundation for the construction and operation of the LIGO Laboratory; the Science and Technology Facilities Council of the United Kingdom, the Max-Planck-Society, and the State of Niedersachsen/Germany for support of the construction and operation of the GEO600 detector; the Italian Istituto Nazionale di Fisica Nucleare and the French Centre National de la Recherche Scientifique for the construction and operation of the Virgo detector; and the Japan Society for the Promotion of Science (JSPS) Core-to-Core Program A, Advanced Research Networks, and Grant-in-Aid for Specially Promoted Research of the KAGRA project. This document has been assigned LIGO document number LIGO-P1400153.

References

- [1] Abadie J *et al.* 2010 *Classical and Quantum Gravity* **27** 173001+
- [2] Ade P *et al.* (BICEP2 Collaboration) 2014 *Phys. Rev. Lett.* **112**(24) 241101
- [3] Hulse R A and Taylor J H 1975 *Astrophys. J. Lett.* **195** L51–L53
- [4] Weisberg J M and Taylor J H 2005 *Binary Radio Pulsars (Astronomical Society of the Pacific Conference Series vol 328)*
- [5] Danzmann K and the LISA study team 1996 *Classical and Quantum Gravity* **13** A247
- [6] Hobbs G *et al.* 2010 *Classical and Quantum Gravity* **27** 084013+

- [7] Weber J 1960 *Physical Review Online Archive (Prola)* **117** 306–313
- [8] Weiss R 1972 Electromagnetically Coupled Broadband Gravitational Antenna Tech. Rep. MIT
- [9] Forward R L 1978 *Physical Review D* **17** 379–390
- [10] Shoemaker D, Schilling R, Schnupp L, Winkler W, Maischberger K and Rüdiger A 1988 *Phys. Rev. D* **38**(2) 423–432
- [11] Robertson D I, Morrison E, Hough J, Killbourn S, Meers B J, Newton G P, Robertson N A, Strain K A and Ward H 1995 *Review of Scientific Instruments* **66** 4447–4452
- [12] Livas J, Benford R, Dewey D, Jeffries A, Linsay P, Saulson P, Shoemaker D and Weiss R 1985 (*Proc. of the Fourth Marcel Grossmann Meeting on General relativity*) 581+
- [13] Abramovici A *et al.* 1996 *Physics Letters A* **218** 157–163
- [14] Abbott B P *et al.* 2009 *Reports on Progress in Physics* **72** 076901+
- [15] Acernese F *et al.* 2008 *Journal of Optics A: Pure and Applied Optics* **10** 064009+
- [16] Grote H and the LIGO Scientific Collaboration 2010 *Classical and Quantum Gravity* **27** 084003+
- [17] Takahashi R and the TAMA Collaboration 2004 *Classical and Quantum Gravity* **21** S403
- [18] Dwyer S and the LIGO Scientific Collaboration *Journal of Physics: Conference Series* to be published in this issue.
- [19] Acernese F *et al.* (the Virgo Collaboration) *Journal of Physics: Conference Series* to be published in this issue.
- [20] Dooley K L and the LIGO Scientific Collaboration *Journal of Physics: Conference Series* to be published in this issue.
- [21] Akutsu T and the KAGRA Collaboration *Journal of Physics: Conference Series* to be published in this issue.
- [22] Abbott B *et al.* 2008 *The Astrophysical Journal Letters* L45+
- [23] The LIGO Scientific Collaboration and the Virgo Collaboration 2009 *Nature* **460** 990–994
- [24] Harry G M and the LIGO Scientific Collaboration 2010 *Classical and Quantum Gravity* **27** 084006+
- [25] The Virgo Collaboration 2012 Advanced Virgo Technical Design Report VIR-0128A-12
- [26] Uchiyama T *et al.* 2012 *Phys. Rev. Lett.* **108**(14) 141101
- [27] Somiya K 2012 *Classical and Quantum Gravity* **29** 124007+
- [28] Arai K *et al.* 2009 *Classical and Quantum Gravity* **26** 204020+
- [29] Lück H *et al.* 2010 *Journal of Physics: Conference Series* **228** 012012+
- [30] Adhikari R, Fritschel P and Waldman S 2006 Enhanced LIGO Tech. Rep. T060156 LIGO Laboratory
- [31] Fricke T *et al.* 2012 *Classical and Quantum Gravity* **29** 065005+
- [32] Hild S *et al.* 2009 *Classical and Quantum Gravity* **26** 055012+
- [33] Hewitson M, Heinzel G, Smith J R, Strain K A and Ward H 2004 *Review of Scientific Instruments* **75** 4702–4709
- [34] Drever R, Hall J, Kowalski F, Hough J, Ford G, Munley A and Ward H 1983 *Applied Physics B* **31** 97–105
- [35] Saulson P R 1990 *Physical Review D* **42** 2437–2445
- [36] URL <http://gwcenter.icrr.u-tokyo.ac.jp/researcher/parameters>
- [37] URL <https://dcc.ligo.org/LIGO-T0900288/public>
- [38] GEO-HF logbook, p.60 URL <https://intranet.aei.uni-hannover.de/geo600/geohflogbook.nsf/f5b2cbf2a827c0198525624b00057d30/4837a612ac990060c12575ce004e70fd>
- [39] Schutz B F 2011 *Classical and Quantum Gravity* **28** 125023
- [40] Fairhurst S 2011 *Classical and Quantum Gravity* **28** 105021
- [41] Fairhurst S 2009 *New Journal of Physics* **11** 123006
- [42] The LIGO Scientific Collaboration and the Virgo Collaboration 2013 Prospects for Localization of Gravitational Wave Transients by the Advanced LIGO and Advanced Virgo Observatories URL <http://arxiv.org/abs/1304.0670>